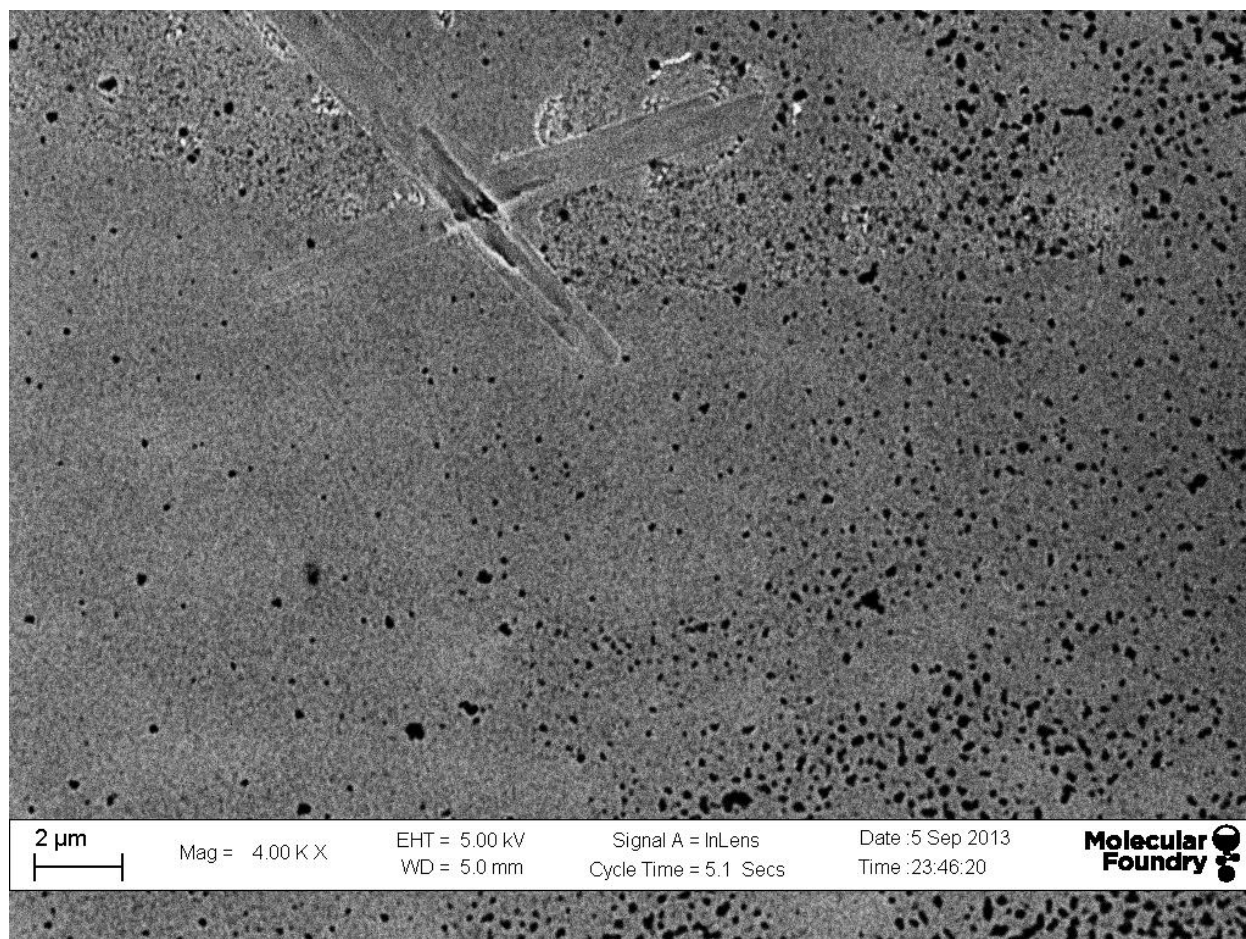
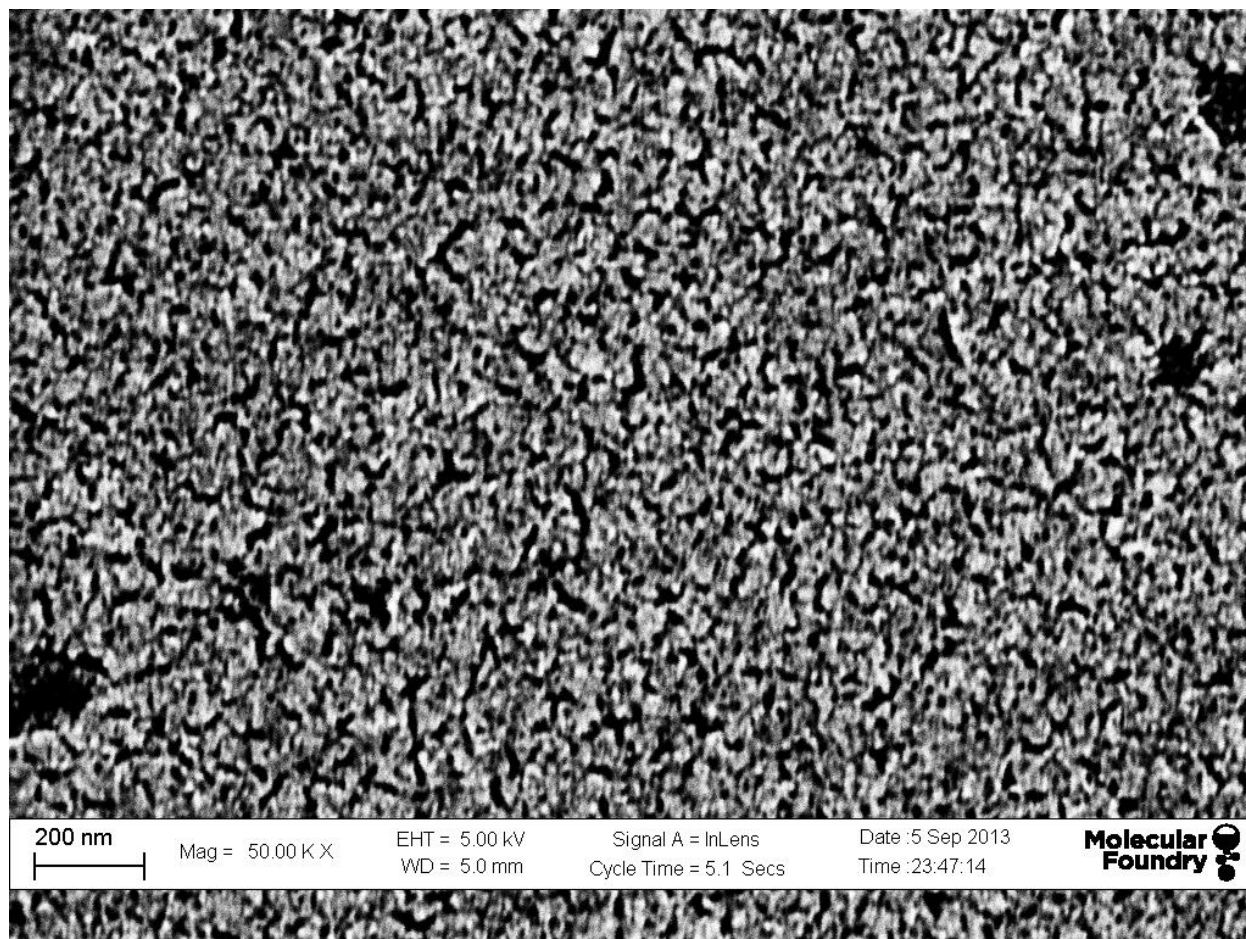


## Supplementary Information



**Figure S1:** Au nanocrystal array exchanged with ammonium thiocyanate scanning electron micrograph at 4kx magnification. The porosity triggered by the exchange is evident, due to the density difference between oleyamine and ammonium thiocyanate.



**Figure S2:** Au nanocrystal array exchanged with ammonium thiocyanate scanning electron micrograph at 50kx magnification. Nanoparticles have fused due to the lack of ligands, as evident from a near-gold like electron conductivity and thermopower.

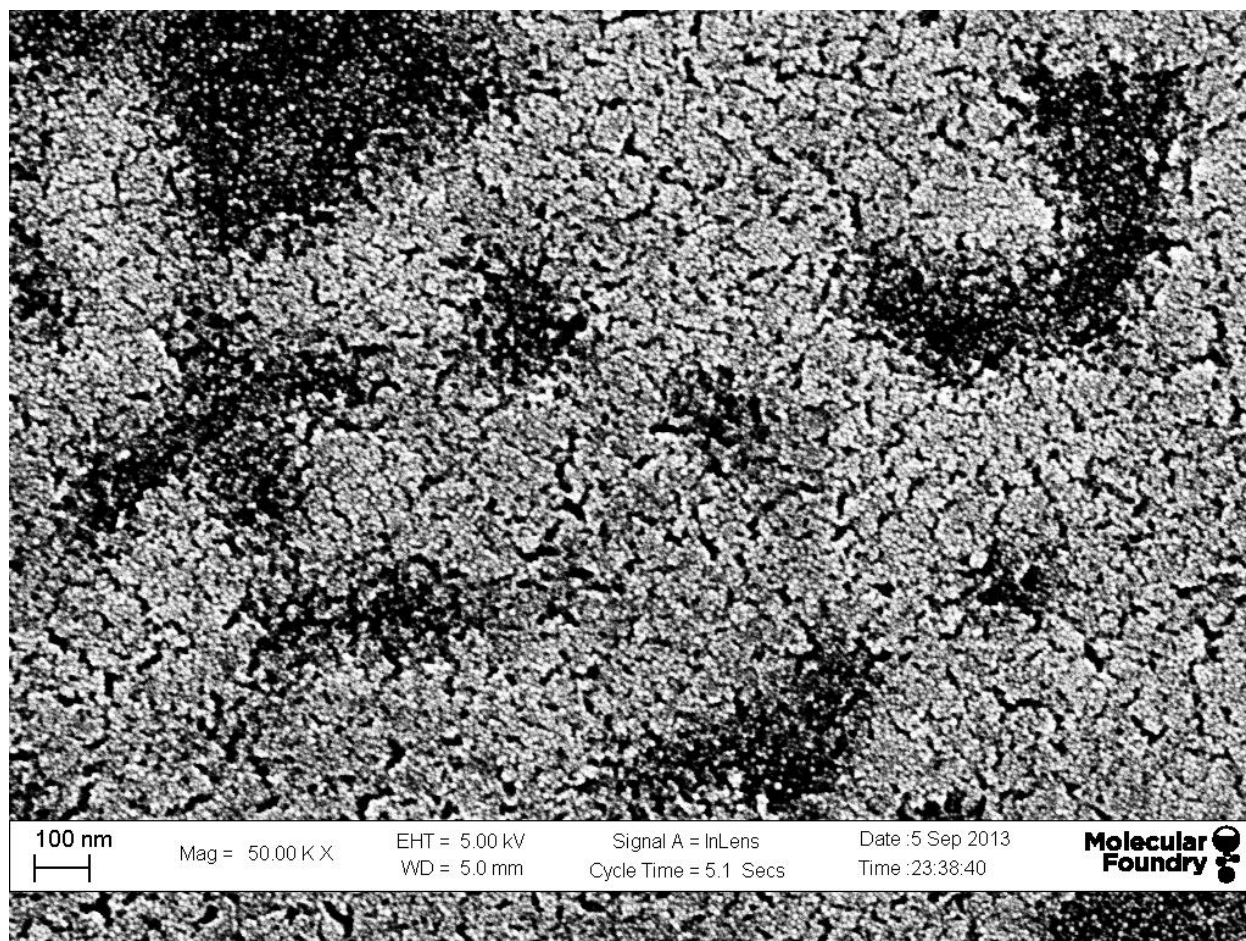


**Figure S3:** Au nanocrystal array exchanged with ethanedithiol scanning electron micrograph at 50kx magnification. Islands are evident on the rough film surface, due to the density change between oleyamine and ethanedithiol.

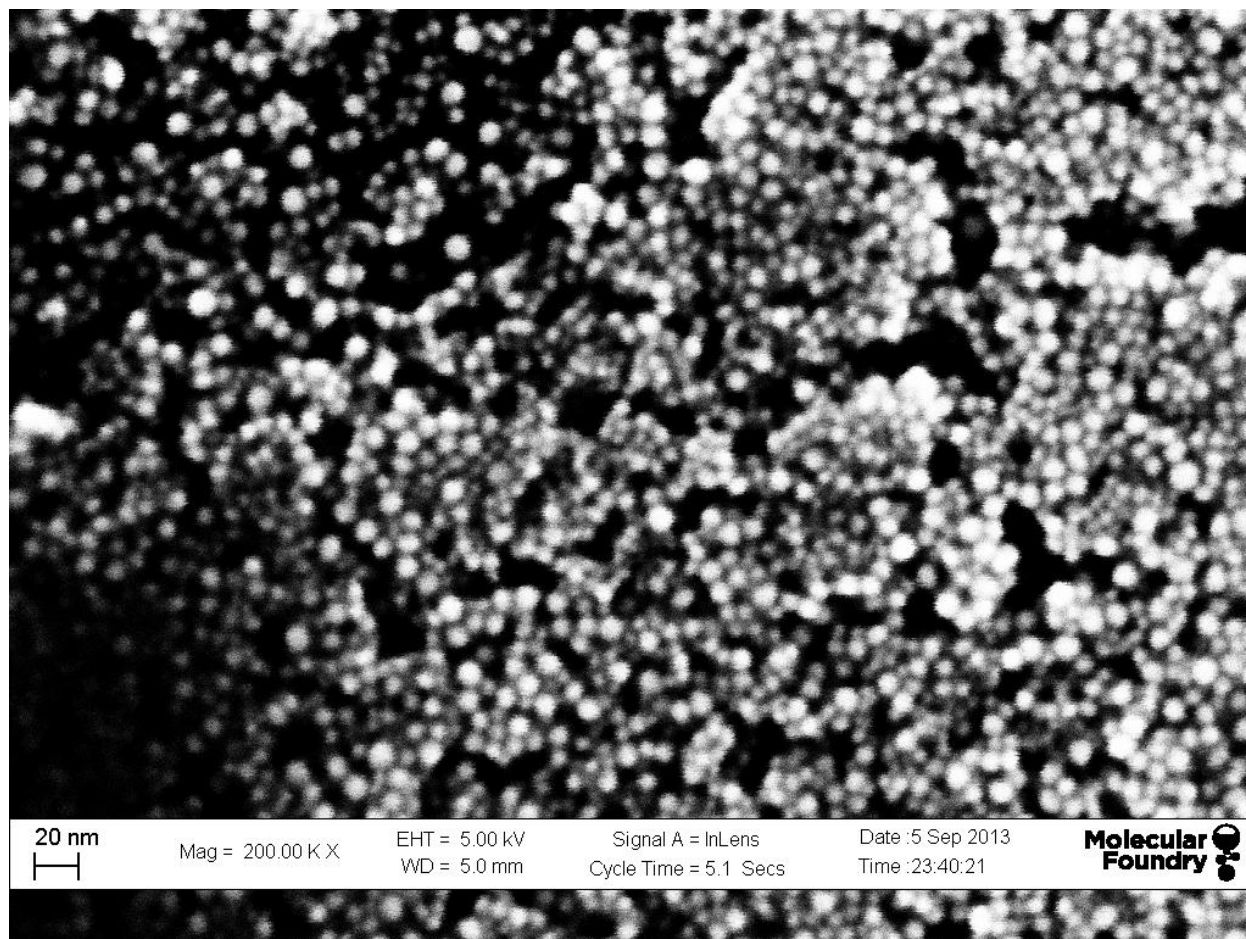


**Figure S4:** Au nanocrystal array exchanged with ethandithiol scanning electron micrograph at 200kx magnification. Distinct nanoparticles are still present in the material. This should mean that the ligand coat is still protecting the nanoparticle, and so transport is dominated by the organic-inorganic interface.

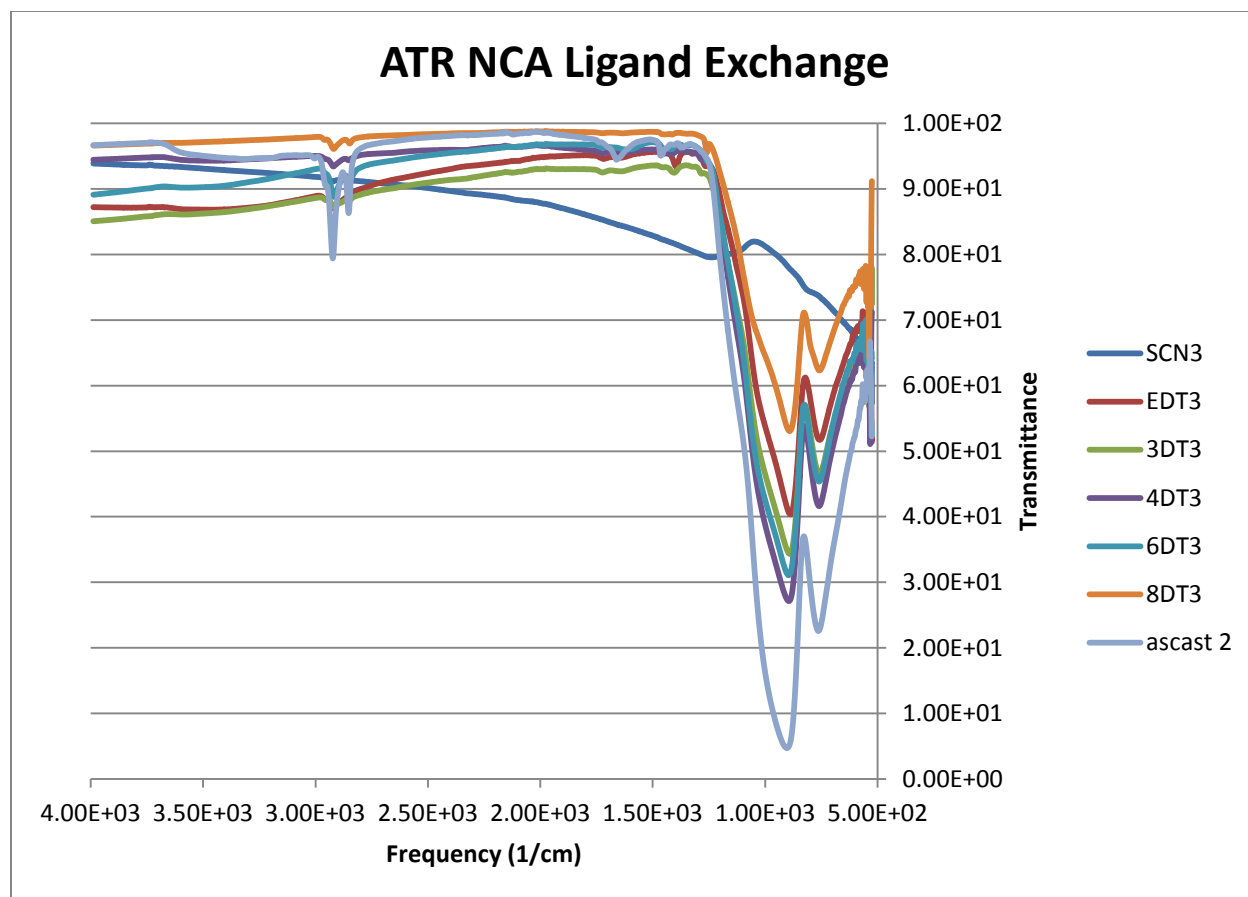


**Figure S5:** This figure demonstrates the difference between an as-cast NCA film with oleyamine, thiocyanate (SCN), and a dithiol. When exchanged with thiocyanate, there are no strong peaks in the FTIR signature. As oleyamine is removed from the nanocrystal surface, the peaks at  $3000\text{ cm}^{-1}$  are reduced in intensity, signifying the removal of the oleyamine.

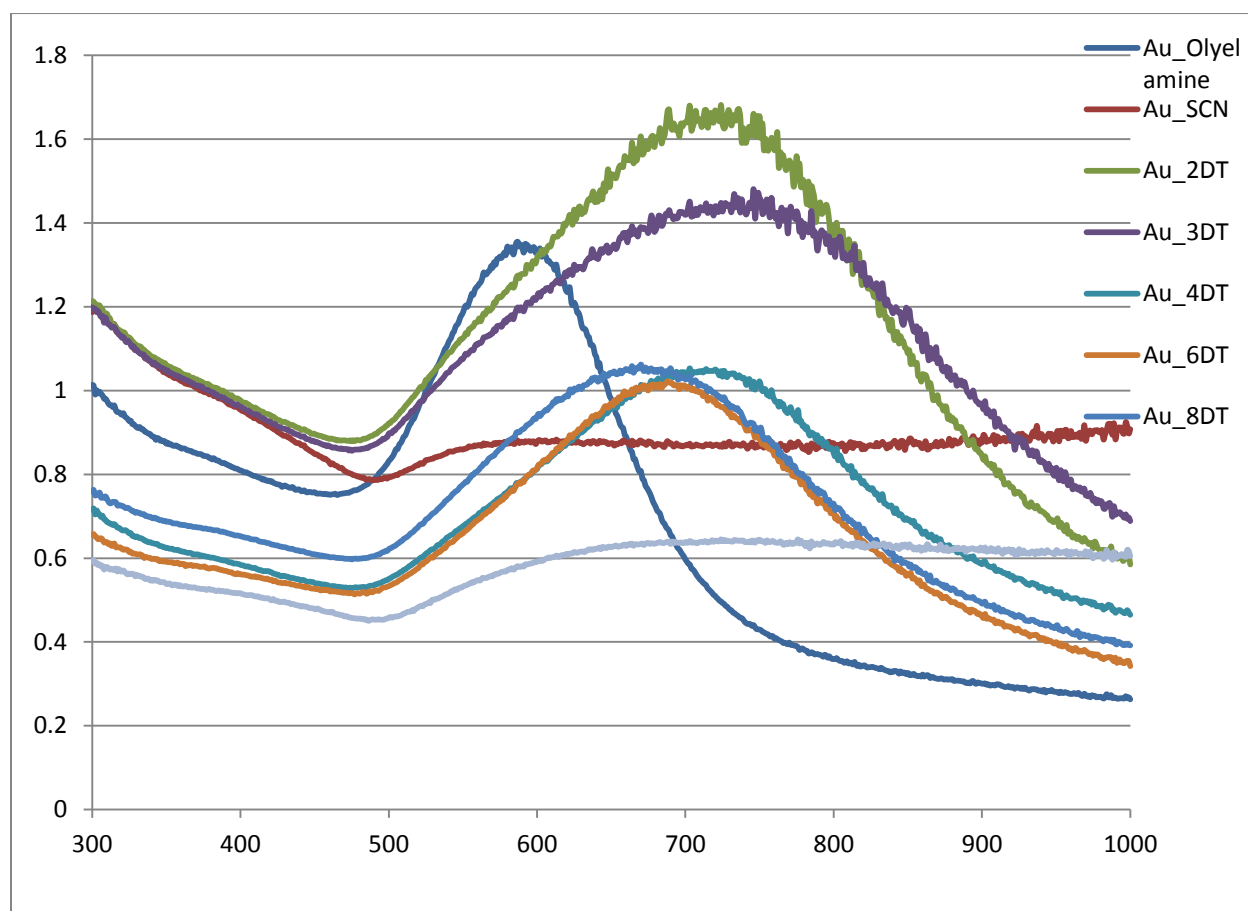


**Figure S6:** The unexchanged oleylamine film shows a peak at 589 nm, corresponding to a photon energy of 2.10 eV. Ethanedithiol and octanedithiol shows a peak at 728nm and 675 nm respectively, translating to a photon energy of 1.70eV and 1.83eV. Interestingly, there is no strong peak in the acetone washed gold NCAs. The observed peaks in the UV-Vis for nanoparticles with oleylamine correspond well with nanoparticles in a thin film geometry affected by the dielectric constant of glass. The shifting surface plasmon resonance (SPR) peaks in the UV-Vis signal to a higher wavelength for NCAs exchanged with octanedithiol and ethanedithiol is due to the nanoparticle aggregation and ripening.

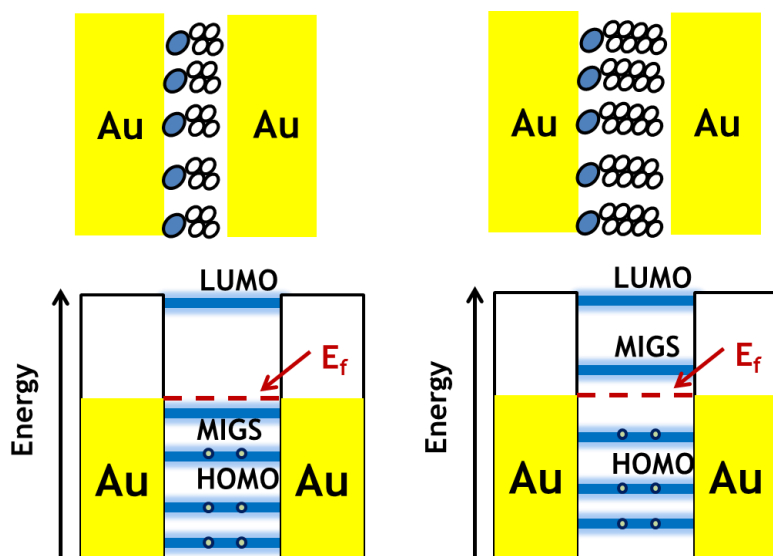


**Figure S7:** Qualitative comparison of electron transport properties in alkanethiol molecular junctions containing shorter ligands versus longer ligands. (Left) Electron tunneling through short alkanethiols with a metal induced gap state below the Fermi energy of gold, resulting in p-type transport (Right) Electron tunneling through longer alkanethiols through the molecular metal induced gap state (MIGS) energy level above the Fermi energy of gold, resulting in n-type behavior.

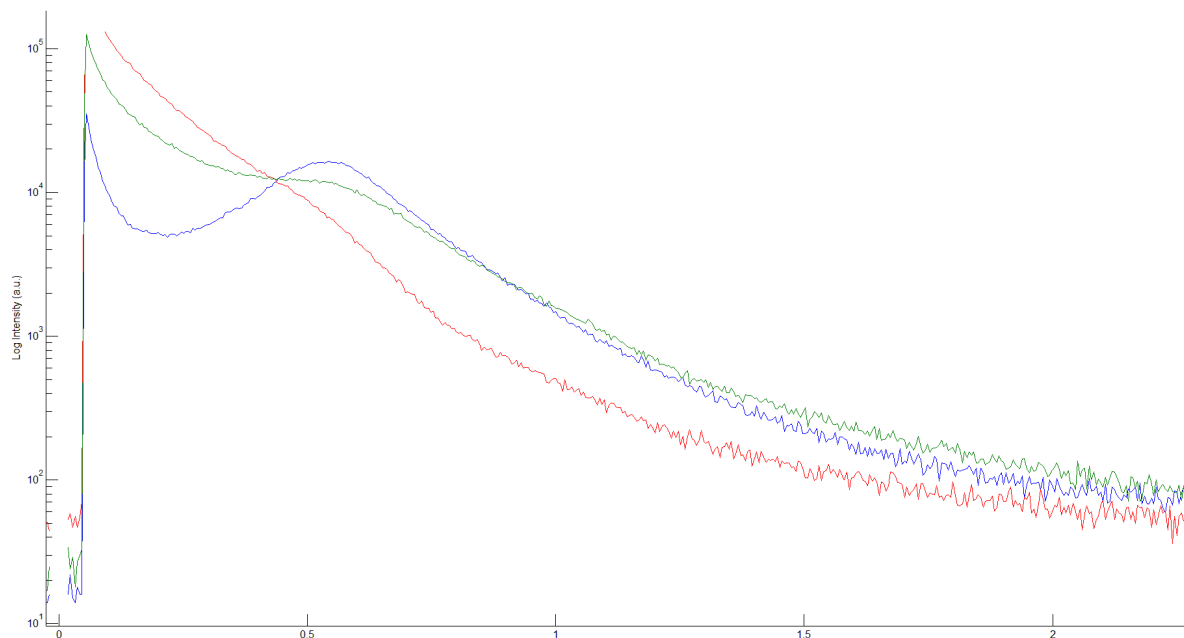


**Figure S8:** Small angle x-ray scattering of Au NCA exchanged with SCN (red), butanedithiol (green) and as-cast (blue). The first peak at  $q = 0.55$  (blue) corresponds to the inter-particle distance in the as-cast film. This distance becomes distorted as the ligands are removed, as shown when exchanged with SCN (red). The lack of a peak shows a large variability in the interparticle spacing, where some nanocrystals may be touching. When exchanged with butanedithiol, the interparticle spacing is somewhat retained, but as the peak becomes less intense, the film is more disordered.

$$N = \frac{SA_{Gold\ NP}}{A_{Sulfur\ Atom}} = \frac{4\pi r_{Gold\ NP}^2}{\pi r_{Sulfur}^2} = \frac{1.13e^{-16}m^2}{3.14e^{-20}} = 3598$$

**Equation 1:** Calculation for number of molecules on surface. This assumes roughly 1/3 participate in charge transport, resulting in ~1000 molecules. Gold Nanoparticle radius is 3 nm, sulfur atom radius is 0.1 nm.

**Table 1:** Molecular lengths

Molecule	Length in Spartan '14 (Å)
Ethanedithiol	7.5
Propanedithiol	8.7
Butanedithiol	9.8
Hexanedithiol	11.5
Octanedithiol	14.0
Benzenedithiol	8.5
Biphenyldithiol	12.2
Terphenyldithiol	16.5
Thiocyanate	3.9
Ethanethiol	4.6
Propanethiol	5.7
Butanethiol	7.0
Pentatethiol	8.2